

# One-step radiation-induced construction of multi-responsive self-assemblies using simple cyclic ethers†

Cite this: *Soft Matter*, 2013, 9, 5959

Chuhong Yu,<sup>a</sup> Li Zhao,<sup>b</sup> Shuojue Wang,<sup>a</sup> Zhenpeng Cui,<sup>a</sup> Jing Peng,<sup>\*a</sup> Jiuqiang Li,<sup>a</sup> Maolin Zhai<sup>\*a</sup> and Jianbin Huang<sup>\*b</sup>

A general and one-step method was developed as a versatile route to fabricate 'smart' self-assemblies via  $\gamma$ -irradiation of simple cyclic ethers under air atmosphere. Only by one-step irradiation in water, a series of amphiphilic oligomers containing oligo(ethylene glycol) (oligo-EG) side chains and their supramolecular assemblies with plentiful morphologies could be prepared, including flower-shaped aggregates, microsphere aggregates, well-defined core-shell micelles and nano-sized capsules. The morphology of the supramolecular assemblies could be facilely adjusted based on the different structures of the cyclic ethers. Moreover, the core-shell micelles prepared by irradiating dicyclohexano-18-crown-6 (DCH18C6) aqueous solutions could be easily controlled by simple external stimulations, such as varying temperature, pH and adding metal ions. Based on the results of a series of cyclic ethers, it is expected that this work can provide a novel and general approach to design and construct 'smart' supramolecular assemblies for biomedical and industrial applications.

Received 31st January 2013

Accepted 16th April 2013

DOI: 10.1039/c3sm50327e

[www.rsc.org/softmatter](http://www.rsc.org/softmatter)

## Introduction

Stimuli-responsive supramolecular assemblies have been widely studied in recent years as promising materials in various fields of materials science and biomedicine, such as targeted drug and gene delivery,<sup>1–5</sup> chemical sensors,<sup>6</sup> and catalysis.<sup>7</sup> The major characteristic of these 'smart' supramolecular assemblies is the capability of responding to small variations in environmental conditions with large and abrupt changes in shape, volume, mechanical and surface properties.<sup>1,8–15</sup> So far, a variety of 'smart' supramolecular objects with different morphologies have been constructed by self-assembly including ellipsoids, disks, cylinders, vesicles, and core-shell structures,<sup>10,16–19</sup> namely those that combine different functionalities of the core and shell.

Stimuli-responsive amphiphilic copolymers are one kind of important self-assembling species known for their flexible and reversible property transitions with external stimulations.<sup>12,13,16,17,20</sup> In particular, poly(ethylene glycol)-like (PEG-

like) amphiphilic copolymers that consist of various kinds of hydrophobic backbones and pendant oligo(ethylene glycol) (oligo-EG) side chains have attracted a great deal of research interest because of their temperature responsiveness and biocompatibility, which have great potential in biomedical and pharmaceutical applications.<sup>21,22</sup> Furthermore, one of the emerging research interests related to the 'smart' material fabrication is the preparation of multi-responsive amphiphilic copolymers.<sup>22–24</sup> When these multi-responsive copolymers are used, the resultant self-assemblies can respond to different stimulations simultaneously, which is a significant and ubiquitous characteristic in nature.

Despite interesting studies reported on the 'smart' self-assemblies preparation using multi-responsive amphiphilic copolymers, the previous synthesis procedures of these copolymers are multi-step and inconvenient.<sup>16,25</sup> Furthermore, the controlled polymerization techniques and extreme experimental conditions are commonly required, such as appropriate initiators, particular chain transfer agents, strict control of monomer ratios, anhydrous and oxygen free conditions. All of these can be time-consuming and complicated, which will restrict the exploitation of these synthesis procedures to practical applications. On the other hand, the 'smart' assemblies constructed from multi-responsive amphiphilic oligomers have seldom been reported. Compared with the corresponding polymers, more consideration should be given to deal with the backbone end groups of the oligomers introduced by the initiators or chain transfer agents. These end groups would bring unexpected effects to the stimuli-responsiveness and self-assembly of the prepared oligomers.<sup>22</sup> For example, when the molar masses were

<sup>a</sup>Beijing National Laboratory for Molecular Sciences (BNLMS), Department of Applied Chemistry and the Key Laboratory of Polymer Chemistry and Physics of the Ministry of Education, College of Chemistry and Molecular Engineering, Peking University, Beijing 100871, P. R. China. E-mail: [jpeng@pku.edu.cn](mailto:jpeng@pku.edu.cn); [mlzhai@pku.edu.cn](mailto:mlzhai@pku.edu.cn); Fax: +86-10-62753794; Tel: +86-10-62757193

<sup>b</sup>Beijing National Laboratory for Molecular Sciences (BNLMS), State Key Laboratory of Structural Chemistry of Unstable and Stable Species, College of Chemistry and Molecular Engineering, Peking University, Beijing 100871, P. R. China. E-mail: [JBHuang@pku.edu.cn](mailto:JBHuang@pku.edu.cn); Fax: +86-10-62751708; Tel: +86-10-62753557

† Electronic supplementary information (ESI) available. See DOI: 10.1039/c3sm50327e

lower, the cloud point (CP) temperatures and micellar structures of the PEO-like copolymers were obviously influenced by the hydrophobicity of the backbone end groups.<sup>26</sup> Therefore, an alternative strategy for constructing 'smart' self-assemblies *via* a facile and general synthesis approach from multi-responsive copolymers is currently desirable.

As a convenient technique,  $\gamma$ -irradiation has been used to generate novel polymeric materials that are useful in therapeutic and technological applications.<sup>27,28</sup> Considering the reactive radicals generated during  $\gamma$ -irradiation, the polymerizations can be carried out efficiently under ambient conditions and without any 'synthetic' steps.<sup>29</sup> However, as a facile synthesis method of 'smart' supramolecular objects,  $\gamma$ -irradiation is not applied to the direct synthesis from simple and small molecules.

In this work, a novel, general and 'one-step  $\gamma$ -irradiation' method was described for the construction of 'smart' self-assemblies directly from different kinds of simple cyclic ethers. After irradiation in water, the cyclic ethers were converted completely to water-soluble amphiphilic oligomers with a hydrophobic poly(vinyl ether) backbone, hydrophilic oligo-EG side chains and end groups (COOH and OH groups). Furthermore, the amphiphilic oligomers simultaneously self-assembled to form supramolecular objects. Since no initiators and catalysts are used, this method does not involve any further treatment, such as a dialysis process for removing the residues. Notably, the structure of the oligo-EG side chains and the hydrophilicity of the oligomers can be easily adjusted based on the structure of the cyclic ethers. Thereby, the morphology and properties of the self-assemblies can also be easily designed using this method. This is a unique and simple route, which is different from all the techniques available in the literatures to the best of our knowledge.

## Experimental

### Synthesis

**Materials.** Dicyclohexano-18-crown-6 (DCH18C6) (98.0% mixture of *cis-syn-cis* and *cis-anti-cis* isomers, Tokyo Chemical Industry Co., Ltd), 18-crown-6 (18C6), 1,4-dioxane (1,4-6C2), tetrahydropyran (99%, Acros Organics Co., Ltd) and other materials were purchased commercially. All chemicals were analytical pure reagents, and used as received.

**Preparation of the self-assemblies.** Typically, the 0.01 M DCH18C6 aqueous solution was irradiated under air atmosphere using a <sup>60</sup>Co  $\gamma$ -source at room temperature. The dose rate was 30.0 Gy min<sup>-1</sup>. The irradiation time varied in the range of 5–60 h. The other cyclic ether aqueous solutions were irradiated under the same conditions.

### Characterization

**Transmission electron microscopy (TEM).** TEM measurements were carried out with a Tecnai F20 transmission electron microscopy operating at 200 kV. One drop of the samples was placed onto a carbon Formvar-coated copper grid, and the excess water was removed with a piece of filter paper. The

samples were then allowed to dry in ambient air at room temperature before TEM observation.

**Dynamic laser scattering (DLS).** The hydrodynamic diameter ( $D_h$ ) of the micelles was determined by a Nano ZS Zetasizer equipped with a He/Ne laser light source (633 nm, 4.0 mW). The measurements were made at a scattering angle of 90°. Before each data collection, the samples were allowed to equilibrate for 2 min at each temperature. The stock solutions were filtered through a Millipore 0.45  $\mu$ m PVDF filter into a dust-free vial. The mean particle size was determined by the intensity of particles and the polydispersity index (PDI) was obtained by the cumulant method.

**Gas chromatography (GC).** Unlike DCH18C6 and small molecular radiolysis products, the resultant oligomers could not be dissolved in nonpolar solvent, such as *n*-heptane. Thus, 0.01 M DCH18C6 aqueous solutions after irradiation were dried at room temperature, and the obtained solid was immersed in a specific amount of *n*-heptane for more than 24 h. The concentration of residual DCH18C6 was determined by GC with a DB-5MS capillary column (30 m  $\times$  0.25 mm i.d., the film thickness is 0.25  $\mu$ m). The injector port was heated to 250 °C. The column temperature was typically programmed as follows: 60 °C for 2 min, 10 °C min<sup>-1</sup> up to 300 °C, and held at 300 °C for 10 min. The temperature of the flame ionization detector was 320 °C.

**Gel permeation chromatography (GPC).** The number-average molecular weight ( $M_n$ ), the weight-average molecular weight ( $M_w$ ) and the polydispersity index (PDI) of the oligomers were determined by GPC, which was performed with a Waters HPLC system using DMF as an eluent. The separation was performed on Waters Styragel HR4 and HR6 columns (7.8 mm  $\times$  300 mm) at 27 °C with a flow rate of 1 ml min<sup>-1</sup>. Monodisperse polymethylmethacrylate standards were used to calibrate the molecular weights.

**Micro-Fourier transform infrared (Micro-FTIR) spectroscopy.** Micro-FTIR spectra were recorded at room temperature with a resolution of 4 cm<sup>-1</sup> by a Micro-FTIR spectrometer (Nicolet iN10 MX).

**<sup>1</sup>H Nuclear magnetic resonance (<sup>1</sup>H NMR) spectroscopy.** <sup>1</sup>H NMR spectra were recorded on a Bruker Avance III 500 MHz NMR spectrometer, using DMSO-d<sub>6</sub> as the solvent and TMS as the internal standard.

**X-ray photoelectron spectroscopy (XPS).** XPS spectra were recorded on an AXIS-Ultra Imaging Photoelectron Spectrometer from Kratos Analytical Ltd. using monochromatic Al-K $\alpha$  radiation in a vacuum of  $2 \times 10^{-8}$  Pa and low energy electron flooding for charge compensation. The data were converted into a VAMAS file format and imported into a CASA XPS software package for manipulation and curve fitting.

**Fluorescence spectroscopy.** Fluorescence emission spectra were recorded on a Cary fluorescence spectrophotometer (Varian) at ambient temperature. The emission spectra were recorded in the range of 350–800 nm at an excitation wavelength of 334 nm. A series of samples containing pyrene (kept at 0.14  $\mu$ M) and oligomers of different concentrations were analysed by this method. The solution was allowed to stand at ambient temperature for 1 day for equilibration. The critical micelle concentration (CMC) was determined from a plot of the ratio of fluorescence intensity at 374 and 384 nm *versus* the oligomer concentration.

**Ultraviolet-visible (UV-Vis) spectroscopy.** The turbidity measurements of the resultant aqueous solutions were performed on a U-3010 UV-Vis spectrophotometer (Hitachi) at a wavelength of 800 nm, equipped with a temperature controller. The heating rate was set at  $1.0\text{ }^{\circ}\text{C min}^{-1}$ . The CP was defined as the temperature corresponding to the transmittance of an oligomer solution decreased to 80%.

**Extended X-ray absorption fine structure (EXAFS) spectroscopy.** The host-guest complexation structure between the resultant products and  $\text{Sr}(\text{NO}_3)_2$  was determined by EXAFS. The samples were placed in 1 cm square polymethylmethacrylate UV-visible cuvettes with  $7.5\text{ }\mu\text{m}$  Kapton windows for the Sr K-edge X-ray absorption measurements. Fluorescence data were collected simultaneously at ambient temperature using an Ar-filled ionization chamber or a 13-element detector (Canberra), at the Shanghai Synchrotron Radiation Facility (SSRF) source beamline B14W1. This beamline uses a  $\text{Si}(111)$  double crystal monochromator and a Pt mirror for harmonic rejection. The monochromator energy was calibrated against the first inflection point of the K-edge of the Zr metal ( $17.998\text{ keV}$ ).

## Results and discussion

### Preparation and characterization of the core-shell micelles

Well-defined core-shell assemblies with a  $\langle D_h \rangle$  of 694 nm and narrow distribution were achieved by irradiating DCH18C6 aqueous solution under air atmosphere (Fig. 1). These supramolecular assemblies have a range of promising applications for the property to combine the different functionalities of the core and shell.<sup>23</sup> We propose that the well-ordered organization of this supramolecular structures is most likely from hydrophobic interactions and hydrogen bonds between the prepared amphiphilic oligomers containing oligo-EG side chains. Therefore, the characteristics of the prepared oligomers were investigated in detail. After irradiation, the colourless aqueous solutions of DCH18C6 became slightly pale yellow (the inset of Fig. 2). The effect of irradiation time on the conversion of DCH18C6 is presented in Fig. 2. As can be seen, when the irradiation time was shorter than 27.8 h, the content of DCH18C6 displayed a linear decline from 100% to less than 5%. After 55.6 h of irradiation, almost no DCH18C6 remained in aqueous solution. Furthermore, only a few other species were

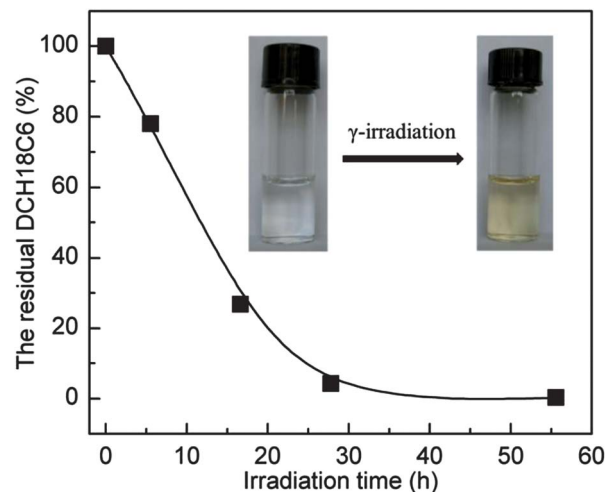


**Fig. 2** The effect of  $\gamma$ -irradiation time on the conversion of DCH18C6. The DCH18C6 content was determined by GC. The inset shows the digital images of the 0.01 M DCH18C6 aqueous solution before and after 55.6 h of  $\gamma$ -irradiation.

produced during irradiation (ESI, Fig. S1<sup>†</sup>), which indicated that the oligomers were prepared efficiently using this method.

The GPC result also confirmed that the oligomers ( $M_n$  ca. 1050) were obtained from DCH18C6 aqueous solution after 55.6 h of irradiation (oligo-DCH18C6) (Table 1). The general structure of oligo-DCH18C6 was investigated by Micro-FTIR,  $^1\text{H}$  NMR and XPS analyses (ESI, Fig. S2–S4 and Table S1<sup>†</sup>), and the results are also shown in Table 1. It is indicated that OH, CHO, and COOH groups are generated as the end groups of side chains, and OH groups are the major end groups, which is consistent with other studies.<sup>30</sup> Additionally, the pH of the DCH18C6 aqueous solution after 55.6 h of irradiation decreased from 5.7 to 3.7. The  $\text{pK}_a$  of oligo-DCH18C6 was determined to be 4.52, which was close to that of carboxylic acid ( $\text{pK}_a \sim 4.80$ ).<sup>31</sup> The CMC of the oligo-DCH18C6 aqueous solution was then determined by measuring the corresponding fluorescence spectra of pyrene as the selected probe. As can be seen, the value of CMC is estimated to be about  $0.40\text{ mg ml}^{-1}$  (Fig. 3). Therefore, the core-shell micelles can be constructed successfully by irradiating DCH18C6 aqueous solution in a one-step process.

### Effect of the cyclic ether structure on the morphology of the self-assemblies

To understand this novel preparation process, three other cyclic ethers with different structures were also used here to fabricate

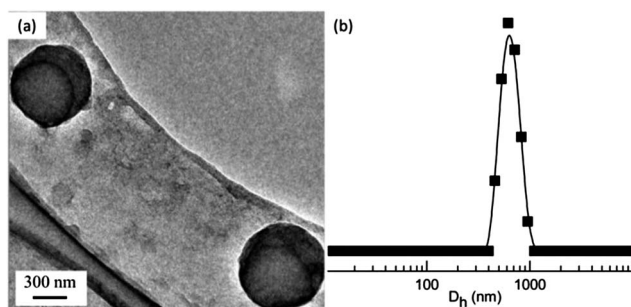


**Fig. 1** TEM image (a) and the corresponding size distribution (b) of the core-shell assemblies obtained by irradiating DCH18C6 aqueous solution for 55.6 h.

**Table 1** Compositions and characteristics of oligo-DCH18C6 obtained from 0.01 M DCH18C6 aqueous solution after 55.6 h of irradiation

$M_n$	PDI	Polymerization degree	The content of side chain end groups (%)		
			OH	CHO	COOH
1050	1.89	2.82 <sup>a</sup>	69.2 <sup>b</sup>	24.6 <sup>b</sup>	5.5 <sup>c</sup>

<sup>a</sup> Calculated by dividing  $M_{\text{DCH18C6}}$  ( $372.5\text{ g mol}^{-1}$ ) from  $M_n$ . <sup>b</sup> Calculated from  $^1\text{H}$  NMR. <sup>c</sup> Calculated from XPS results.

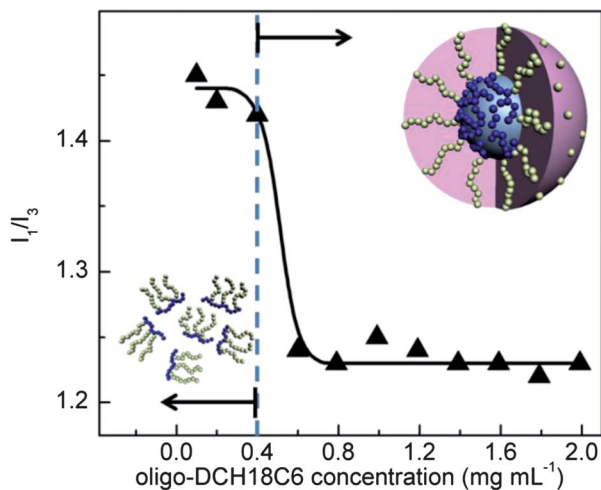


**Fig. 3** Linear plot showing the fluorescence intensity ratio of pyrene at 374 nm ( $I_1$ ) and 384 nm ( $I_3$ ) versus the oligo-DCH18C6 concentration.

supramolecular assemblies by the ‘one-step  $\gamma$ -irradiation’ method. TEM images and DLS results (Fig. 4) revealed that nano-sized or micro-sized assemblies with a narrow size distribution yet with various morphologies were prepared, which indicated that the structure of the cyclic ethers has a dominative effect on the final assembly morphology. The feasible schematic diagram for the ‘one-step  $\gamma$ -irradiation’ method is depicted in Scheme 1.

When exposed to  $\gamma$ -irradiation, the C–O bonds of cyclic ethers would cleave due to the high energy (*ca.* 1.24 MeV) and rearrange

to produce intermediate species containing end C=C groups, which would polymerize to form water-soluble amphiphilic oligomers. Thereby, the oligomers obtained by using this method possess the same backbones. However, different structures of the cyclic ethers lead to different structures and hydrophilicity of the side chains, which will strongly influence the subsequent self-assembly behaviour of the resulting oligomers.

It is worth noting that novel flower-shaped supramolecular assemblies with a  $\langle D_h \rangle$  of 533 nm were formed due to the high hydrophobicity of the side chains in oligo-tetrahydropyran (Fig. 4(a) and (d)). These flower-shaped morphologies were primarily synthesized from copolymers based on PEO and polypeptides.<sup>32,33</sup> To the best of our knowledge, it is the first time to synthesize flower-shaped assemblies in analogous oligomer systems. However, microsphere structures with a  $\langle D_h \rangle$  of 205 nm were formed for oligo-1,4-6C2, and the core-shell structures were not observed (Fig. 4(b) and (e)). It may be attributed to the hydrophilicity of side chains in oligo-1,4-6C2, which is higher than that of oligo-tetrahydropyran, but lower than that of oligo-DCH18C6. Furthermore, nano-sized capsules with a  $\langle D_h \rangle$  of 76 nm were obtained for oligo-18C6 since its hydrophilicity is higher than that of oligo-DCH18C6. In this case, we suggest that the ‘one-step  $\gamma$ -irradiation’ method is applicable to design and prepare supramolecular assemblies with various morphologies by employing a wide range of cyclic ethers.

### Multi-responsive properties of the self-assemblies

**a Thermo-responsive behaviour.** The reversible temperature-triggered aggregation–dissociation behaviour of the

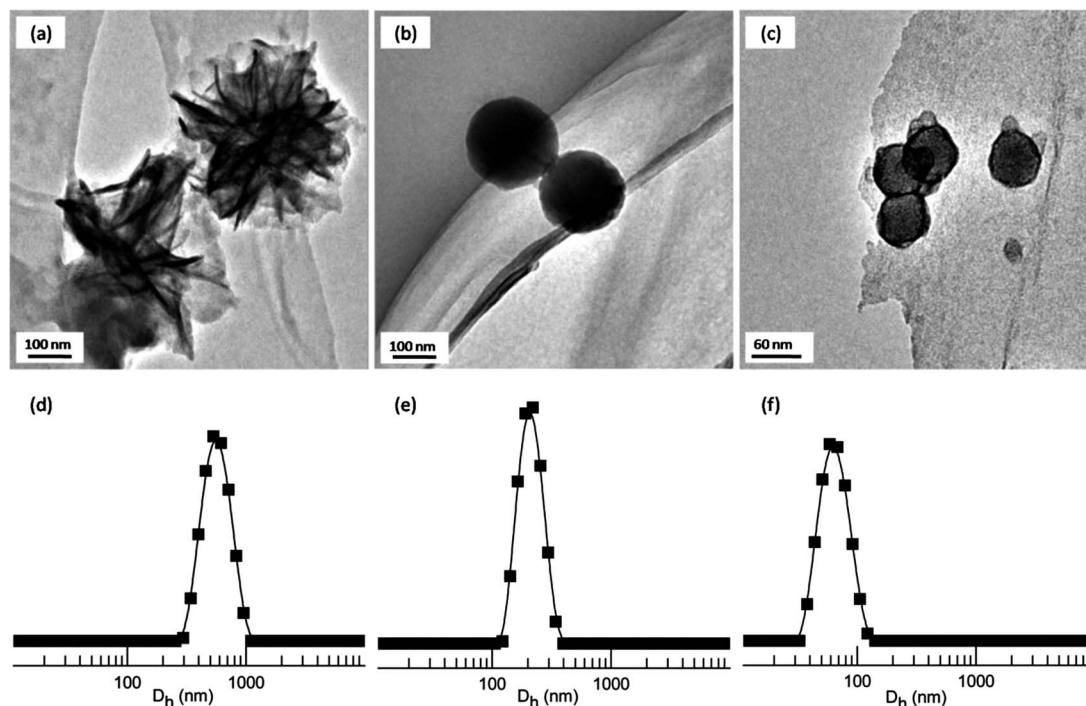
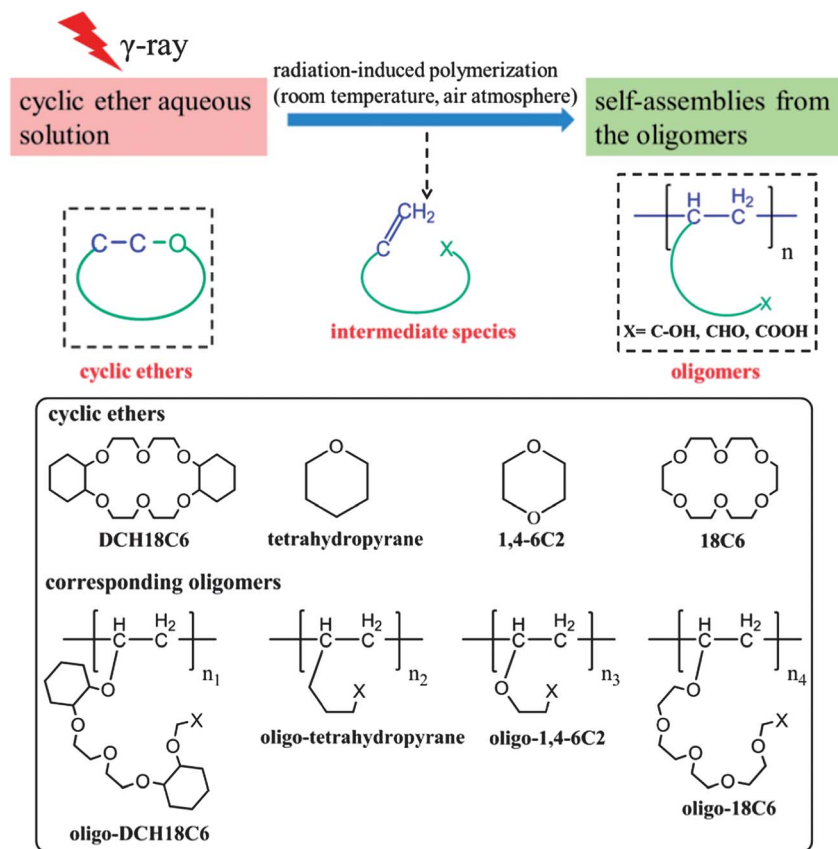


**Fig. 4** TEM images and the corresponding size distributions of the supramolecular assemblies obtained from various cyclic ethers after 55.6 h of irradiation in water: (a) and (d) 0.01 M tetrahydropyran aqueous solution, (b) and (e) 0.01 M 1,4-6C2 aqueous solution, (c) and (f) 0.01 M 18C6 aqueous solution.



**Scheme 1** Schematic representation of the synthesis of self-assemblies from cyclic ethers via the 'one-step  $\gamma$ -irradiation' method.

core-shell micelles obtained from oligo-DCH18C6 was determined by DLS (Fig. 5). At pH 3.7 and a concentration of  $1.99 \text{ mg ml}^{-1}$ , the micelle size remained constant for months at  $25^\circ\text{C}$ . However, the situation was completely different when the solution temperature increased from  $25$  to  $38^\circ\text{C}$ . DLS results showed that the  $\langle D_h \rangle$  of the assemblies increased from  $694$  to  $910 \text{ nm}$ , which was similar to the results of other micelles prepared from 'brush type' polymers containing oligo-EG.<sup>34</sup> The increase in the assembly diameter can be attributed to the aggregation of the micelles because of the weakening of the hydrogen bonds between oligomers and surrounding water molecules. The consequent enhancement of the hydrophobicity of the core-shell micelles promotes the aggregation of the micelles.<sup>22</sup> TEM images also confirmed the formation of larger aggregations at  $38^\circ\text{C}$ . In addition, a few of fusion micelles were observed (ESI, Fig. S5†). However, the diameter of the single core-shell micelle decreased slightly when the temperature increased due to the micelle dehydration. When the temperature decreased back to  $25^\circ\text{C}$ , the complete dissociation of the assemblies was observed, since the hydrogen bonds between oligomers and surrounding water molecules were recovered and the oligomers returned to their highly hydrophilic form. Moreover, as shown in Fig. 5, these aggregation and dissociation processes could be repeated several times without significant deterioration in the aggregation-dissociation kinetics, which shows particular promise for various advanced applications including oil field engineering.<sup>31,35</sup>

**b pH-responsive behaviour.** The core-shell micelles could also be adjusted simply by varying the pH of the aqueous solution due to the alteration of the ionization degree of COOH groups in oligo-DCH18C6 (Fig. 6). The hydrodynamic size of the assemblies decreased with increase of pH and changed dramatically at  $\text{pK}_a$  of oligo-DCH18C6. When the pH is less than 3, oligo-DCH18C6 is completely protonated. Thereby, the hydrogen bonds among ethylene glycol units, OH and COOH groups on the surface of the adjacent particles promoted the formation of compact aggregates. With increase in pH, oligo-DCH18C6 became more hydrophilic because of the deprotonation of the COOH groups. The weakening of the hydrogen bonds but strengthening of the electrostatic repulsions among the adjacent particles certainly led to dispersive assemblies with smaller diameters.

**c Effect of metal ions.** The addition of salt to the aqueous solution of the temperature responsive copolymers generally results in a decrease of the corresponding CP.<sup>22,36</sup> It is well known as the salting-out effect, which influences the hydration of the polymer and leads to a lower phase transition temperature. Interestingly, the presence of different metal ions in the oligo-DCH18C6 aqueous solution shows different effects on the CP. As shown in Fig. 7, the phase transition temperature of oligo-DCH18C6 increased by about  $5^\circ\text{C}$  in the presence of  $0.4 \text{ mM Sr}^{2+}$  or  $\text{K}^+$  (the molar ratio of oligomers to ions is 25), which might be attributed to the salting-in effect. However, the presence of  $0.4 \text{ mM Li}^+$  or  $\text{Mg}^{2+}$  resulted in the obvious salting-out

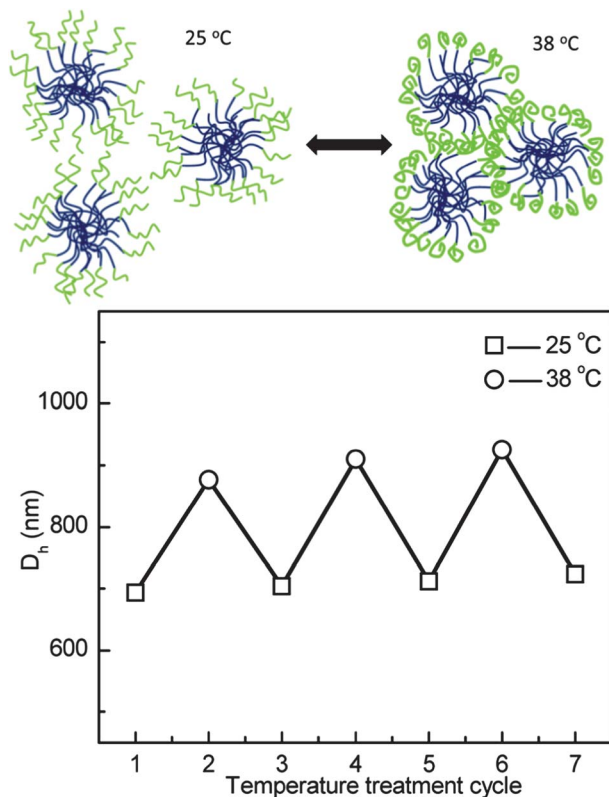


**Fig. 5** The temperature-triggered switch of the aggregation–dissociation of the core–shell micelles obtained from the 1.99 mg ml<sup>-1</sup> of oligo-DCH18C6 aqueous solution.

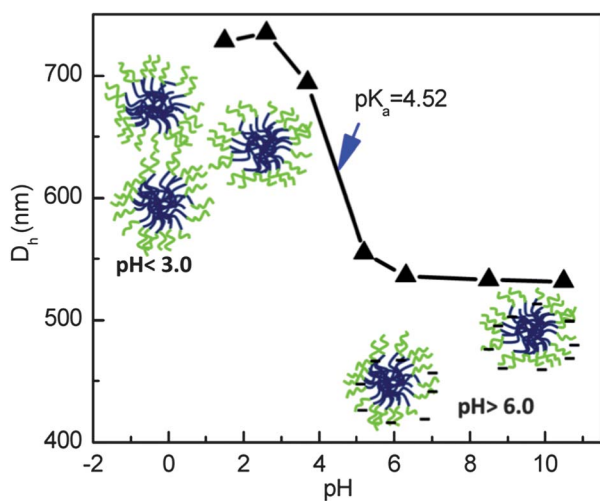


**Fig. 6** pH-dependence of the diameter size of the core–shell micelles obtained from 1.99 mg ml<sup>-1</sup> of oligo-DCH18C6 aqueous solution.

effect, and the CP decreased by more than 5 °C. These differences may be credited to the different complexation behaviours between various metal ions and the side chains of oligo-DCH18C6.

DCH18C6 has been reported as an efficiently selective extractant for Sr<sup>2+</sup>.<sup>30</sup> Thereby, oligo-DCH18C6 is also expected to have potential extraction toward Sr<sup>2+</sup>. The host–guest complex

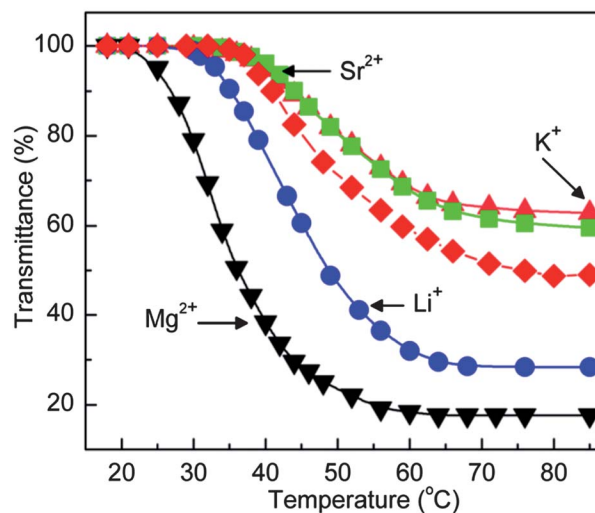
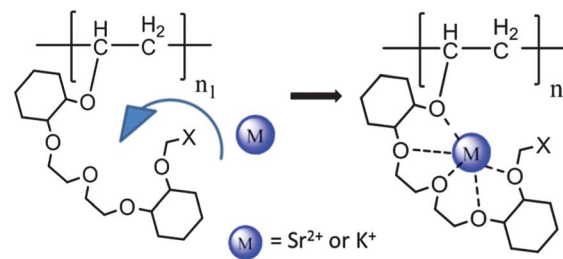


**Fig. 7** Variation of the transmittance of 1.99 mg ml<sup>-1</sup> of oligo-DCH18C6 aqueous solution in the presence of different metal ions as a function of temperature: ▲, ■, ▼ – in the presence of 0.4 mM of K<sup>+</sup>, Sr<sup>2+</sup>, Li<sup>+</sup> and Mg<sup>2+</sup>, respectively; ◆ – in the absence of metal ions.

between oligo-DCH18C6 and Sr<sup>2+</sup> in aqueous solution was confirmed by EXAFS results. Unlike the Sr–O coordination number ( $N_0$ ) between DCH18C6 and Sr<sup>2+</sup>, which is 10 according to both theoretical and experiment data,<sup>36</sup> the  $N_0$  between oligo-DCH18C6 and Sr<sup>2+</sup> is 6.6 (ESI, Table S2†). Moreover, since the complexation ability of the crown ethers is highly dependent on the size of the guest ions, the complexation behaviour of Sr<sup>2+</sup> and K<sup>+</sup> with oligo-DCH18C6 should be analogical due to their similar ionic size. Therefore, the similar effects of K<sup>+</sup> and Sr<sup>2+</sup> on the transmittance of the oligo-DCH18C6 solution were observed in Fig. 7. After the complexation of oligo-DCH18C6 with K<sup>+</sup> or Sr<sup>2+</sup>, the electrical repulsion between positively charged ions prevents the aggregation of the micelles which induces the increase of the phase transition temperature of the oligo-DCH18C6 aqueous solution. In contrast, the addition of Li<sup>+</sup> or Mg<sup>2+</sup>, which has much smaller size, facilitates the polymer–polymer interactions and reduces the CP greatly. All these results demonstrate that the prepared core–shell micelles of oligo-DCH18C6 exhibit excellent sensitivity to metal ions based on the ion size.

## Conclusions

Supramolecular assemblies with plentiful morphologies were prepared *via* a ‘one-step  $\gamma$ -irradiation’ method in water using a series of simple cyclic ethers. By tuning the cyclic ether

structure, various self-assemblies such as flower-shaped aggregates, microsphere aggregates, core-shell micelles and nano-sized capsules were obtained. The core-shell micelles prepared by irradiation of DCH18C6 aqueous solution exhibited reversible temperature-triggered aggregation-dissociation behaviour. The hydrodynamic diameter of the assemblies could also be altered by varying the pH. Furthermore, the addition of metal ions such as  $\text{Sr}^{2+}$  and  $\text{K}^+$  increased the CP of the aqueous solution of the core-shell micelles due to the size-matching selective complexation between metal ions and the oligomers, whereas the addition of  $\text{Li}^+$  and  $\text{Mg}^{2+}$  decreased the CP obviously. Therefore, the core-shell micelles prepared from one-step  $\gamma$ -irradiation of DCH18C6 aqueous solution could be easily controlled by simple stimulations, such as temperature, pH and metal ions. It is expected that this work sheds light on the design and construction of 'smart' materials with more complicated architectures and broad applications based on the 'one-step  $\gamma$ -irradiation' method.

## Acknowledgements

We would like to thank Prof. Xuefeng Fu for her help with the GPC measurement. This work was supported by the National Natural Science Foundation of China (NNSFC, Project no. 11079007, 21073008 and 21273013) and 973 program (Project no. 2013CB933800).

## Notes and references

- 1 M. Lee, S. J. Lee and L. H. Jiang, *J. Am. Chem. Soc.*, 2004, **126**, 12724–12725.
- 2 E. Fleige, M. A. Quadir and R. Haag, *Adv. Drug Delivery Rev.*, 2012, **64**, 866–884.
- 3 X. J. Loh, J. del Barrio, P. P. C. Toh, T. C. Lee, D. Jiao, U. Rauwald, E. A. Appel and O. A. Scherman, *Biomacromolecules*, 2011, **13**, 84–91.
- 4 J. Zhang and P. X. Ma, *Angew. Chem., Int. Ed.*, 2008, **48**, 964–968.
- 5 L. Zhao, Y. Yan and J. Huang, *Langmuir*, 2012, **28**, 5548–5554.
- 6 D. T. McQuade, A. E. Pullen and T. M. Swager, *Chem. Rev.*, 2000, **100**, 2537–2574.
- 7 H. M. Jung, K. E. Price and D. T. McQuade, *J. Am. Chem. Soc.*, 2003, **125**, 5351–5355.
- 8 Y. Chen, X. H. Pang and C. M. Dong, *Adv. Funct. Mater.*, 2010, **20**, 579–586.
- 9 K. S. Moon, H. J. Kim, E. Lee and M. Lee, *Angew. Chem., Int. Ed.*, 2007, **46**, 6807–6810.
- 10 H. J. Kim, T. Kim and M. Lee, *Acc. Chem. Res.*, 2010, **44**, 72–82.
- 11 X. Li, Y. Gao, Y. Kuang and B. Xu, *Chem. Commun.*, 2010, **46**, 5364–5366.
- 12 A. Klaikherd, C. Nagamani and S. Thayumanavan, *J. Am. Chem. Soc.*, 2009, **131**, 4830–4838.
- 13 Y. Zhao, *Macromolecules*, 2012, **45**, 3647–3657.
- 14 T. Fenske, H. G. Korth, A. Mohr and C. Schmuck, *Chem.–Eur. J.*, 2012, **18**, 738–755.
- 15 J. Rubio, I. Alfonso, M. I. Burguete and S. V. Luis, *Soft Matter*, 2011, **7**, 10737–10748.
- 16 X. Yan, F. Wang, B. Zheng and F. Huang, *Chem. Soc. Rev.*, 2012, **41**, 6042–6065.
- 17 E. R. Gillies, T. B. Jonsson and J. M. J. Fréchet, *J. Am. Chem. Soc.*, 2004, **126**, 11936–11943.
- 18 J. Hao and H. Hoffmann, *Curr. Opin. Colloid Interface Sci.*, 2004, **9**, 279–293.
- 19 Y. Liu, Y. Yu, J. Gao, Z. Wang and X. Zhang, *Angew. Chem.*, 2010, **122**, 6726–6729.
- 20 M. A. C. Stuart, W. T. S. Huck, J. Genzer, M. Müller, C. Ober, M. Stamm, G. B. Sukhorukov, I. Szleifer, V. V. Tsukruk and M. Urban, *Nat. Mater.*, 2010, **9**, 101–113.
- 21 H. Otsuka, Y. Nagasaki and K. Kataoka, *Adv. Drug Delivery Rev.*, 2012, **64**, 246–255.
- 22 C. Weber, R. Hoogenboom and U. S. Schubert, *Prog. Polym. Sci.*, 2012, **37**, 686–714.
- 23 O. J. Cayre, N. Chagneux and S. Biggs, *Soft Matter*, 2011, **7**, 2211–2234.
- 24 L. Zha, B. Banik and F. Alexis, *Soft Matter*, 2011, **7**, 5908–5916.
- 25 J. F. Lutz, *J. Polym. Sci., Part A: Polym. Chem.*, 2008, **46**, 3459–3470.
- 26 F. D. Jochum, L. Zur Borg, P. J. Roth and P. Theato, *Macromolecules*, 2009, **42**, 7854–7862.
- 27 C. He, K. Jiao, X. Zhang, M. Xiang, Z. Li and H. Wang, *Soft Matter*, 2011, **7**, 2943–2952.
- 28 X. Wang, H. Wang and H. R. Brown, *Soft Matter*, 2010, **7**, 211–219.
- 29 M. Bassetti, I. Fratoddi, L. Lilla, C. Pasquini, M. Vittoria Russo and O. Ursini, *J. Polym. Sci., Part A: Polym. Chem.*, 2012, **50**, 5097–5106.
- 30 C. Yu, J. Peng, J. Li and M. Zhai, *Radiat. Phys. Chem.*, 2012, **81**, 1736–1740.
- 31 R. T. Woodward, C. Hight, U. Yildiz, N. Schaeffer, E. M. Valliant, J. R. Jones, M. M. Stevens and J. V. M. Weaver, *Soft Matter*, 2011, **7**, 7560–7566.
- 32 V. K. Kotharangannagari, A. Sánchez-Ferrer, J. Ruokolainen and R. Mezzenga, *Macromolecules*, 2011, **44**, 4569–4573.
- 33 K. Inomata, M. Kasuya, H. Sugimoto and E. Nakanishi, *Polymer*, 2005, **46**, 10035–10044.
- 34 C. Li, C. Lavigneur and J. X. X. Zhu, *Langmuir*, 2011, **27**, 11174–11179.
- 35 M. Grzelczak, J. Vermant, E. M. Furst and L. M. Liz-Marzán, *ACS Nano*, 2010, **4**, 3591–3605.
- 36 M. P. Jensen, J. A. Dzielawa, P. Rickert and M. L. Dietz, *J. Am. Chem. Soc.*, 2002, **124**, 10664–10665.